ACS Catalysis

Open Access

pubs.acs.org/acscatalysis

Research Article

Visible-Light-Mediated Pyridine-*N*-oxide-Assisted Alkoxycarbonyl Chlorination of Alkenes via Iron-Catalyzed Radical Ligand Transfer

Mangish Ghosh,[§] Tirtha Mandal,[§] Zen Shimizu, and Oliver Reiser*

Cite This: https://doi.org/10.1021/acscatal.6c03087

Read Online

ACCESS | Metrics & More | Article Recommendations | Supporting Information

ABSTRACT: The scalable, catalytic alkoxycarbonylchlorination of alkenes from alkyloxalyl chlorides, generated *in situ* from oxalyl chlorides and alcohols, by a combination of 4-cyanopyridine-*N*-oxide and Fe(II)-bipyridine has been developed. A broad range of functional groups is tolerated with high regio- and chemoselectivity. The breadth of this protocol is demonstrated by the successful engagement of activated and unactivated alkenes, including late-stage functionalization of alkenes containing pharmacophores. Control experiments and mechanistic investigations, such as NMR, EPR, and radical trapping analyses, indicate that the *in situ*-formed alkyloxalyl chloride-pyridine-*N*-oxide adduct undergoes decarboxylative photoinduced N−O bond fragmentation to generate acyl radicals, whereas the Fe(II) catalyst acts as a redox-neutral electron shuttle and assists chloride transfer via a radical ligand transfer (RLT) pathway.

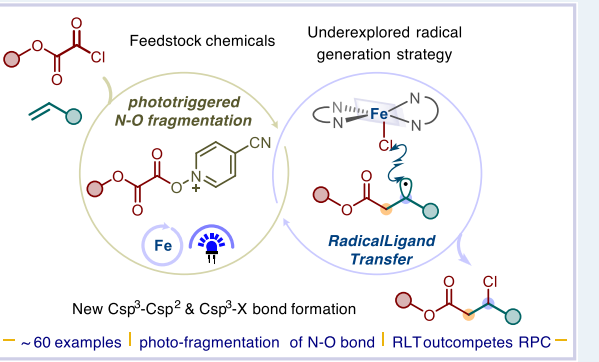

KEYWORDS: *atom-transfer radical addition, alkoxycarbonylchlorination, radical ligand transfer, iron catalysis, pyridinium ester, β-chloroesters*

INTRODUCTION

Atom-transfer radical addition (ATRA) reactions, pioneered by Kharasch, are linchpin transformations in synthetic chemistry, enabling the difunctionalization of unsaturated moieties with high atom and step economy.[1,2] As common ATRA reactions of early days required harsh reaction conditions and toxic or hazardous reagents and were hampered by limited functional group tolerance, the upsurge of photoredox catalysis has led to a resurgence of this transformation, obviating the shortcomings mentioned above.[3−14] While organic Csp^3-X (X = halides, azides, thiocyanates, etc.) precursors are well-established antecedents in metallaphotoredox (MLCT mode of activation)[13−18] ATRA processes, the photoactivation of Csp^2-X molecules is underexplored (Figure 1A).[19−21] Recently, we developed ATRA reactions of aroyl chlorides using a heteroleptic Cu(I) complex (Figure 1B), which could efficiently perform the β-chloroacylation of olefins owing to its adaptive ligand environment being tailored for the distinctive mechanistic steps catalyzed by the Cu(I) and Cu(II) redox couple.[22] The success of this strategy relied on the facile formation of a phosphine-bound bridged Cu(I)-Cl species, which enabled SET of aroyl chlorides (Figure 1B). We questioned whether readily available and inexpensive alkyloxalyl chlorides could also serve as radical precursors, released via a heteroleptic Cu(I) catalyst,[23] and thus enable the alkoxycarbonylchlorination of alkenes. Despite this seemingly minor variation, we have been unable to achieve the desired ATRA process with Cu(I) photocatalysts (*cf.* Figures 1B,E).

A state-of-the-art method developed by Stephenson and coworkers employs pyridine *N*-oxides and their derivatives for the activation of acid anhydrides[24,25] and chlorides[26,27] to access a photocleavable pyridinium ester that would deliver carbon-centered radicals either through the redox-triggered fragmentation or via direct light-induced homolysis of the N−O bond (Figure 1C). Moreover, by using a motif derived from an abundant heteroaromatic building block, the designed pyridinium esters feature highly tunable core structures, enabling control over fragmentation events. Building on this precedent, we envisioned that pyridine *N*-oxides could be employed as an activator of alkyloxalyl chlorides to generate auxiliary **I** *in situ*, which would undergo, in a visible-light-induced metal-free fashion, a decarboxylative N−O bond fragmentation to generate a nucleophilic acyloxy radical. This intermediate might be capable of adding to an alkene, leading to the formation of radical **V** (*cf.* Figure 3 for a detailed mechanistic discussion), which was

Received: April 19, 2026
Revised: May 26, 2026
Accepted: May 27, 2026

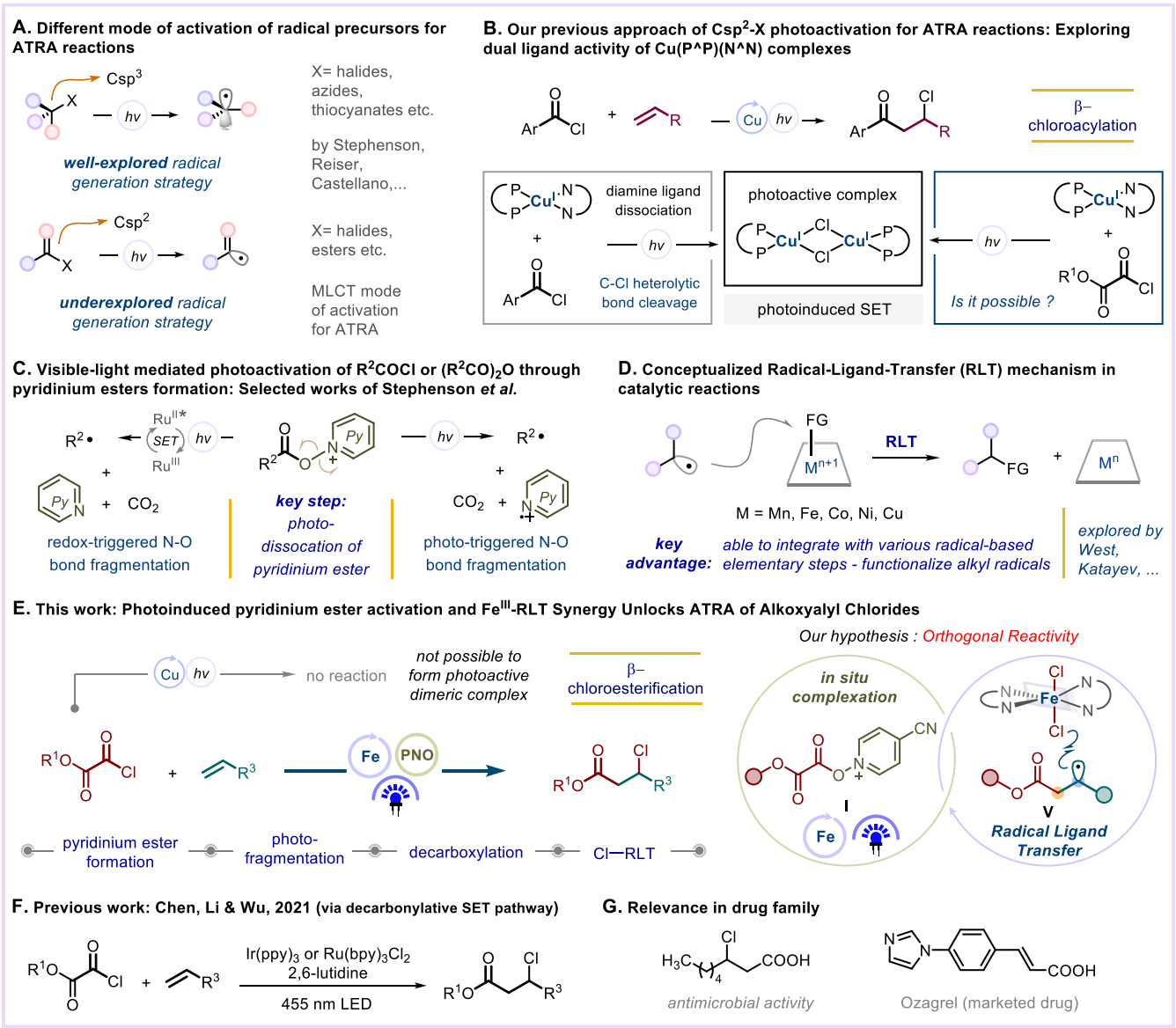

Figure 1. State-of-the-art of the alkoxycarbonyl chlorination of alkenes. (A) Different activation modes of radical precursors used for ATRA reactions. (B) Our previous photoredox catalytic approach for Csp^2-X activation. (C) Precedent for the photoactivation of acyl chlorides using pyridine *N*-oxide. (D) Radical ligand transfer mechanism in photocatalytic reactions. (E) Overview of this work. (F) Previous work on chloroesterification of alkenes.

previously only viable with Ru(II) and Ir(III) polypyridyl photocatalysts and an activator, e.g., 2,6-lutidine (Figure 1F).[28] Interception of an *in situ* photogenerated radical **V** by a ligand transfer (RLT) event[29−36] (Figure 1D) would give rise to the desired β-chloroesters (Figure 1E). Indeed, we identified that catalytic amounts of the Fe(II)-bipyridine complex $[Fe(bpy)_3](NTf_2)_2$[37,38] in combination with pyridine *N*-oxides (**PNO**s) promote the alkoxycarbonylchlorination of activated and unactivated alkenes, leading to the formation of β-chloroesters (Figure 1E).

We posit that photofragmentation of the *in situ* generated pyridinium ester and iron-catalyzed RLT can proceed in an orthogonal yet cooperative manner. This work not only showcases the utility of earth-abundant iron complexes in radical-mediated difunctionalizations but also underscores the broader potential of C(sp^2)-X electrophiles in ATRA-type transformations, thereby opening a rich chemical space with relevance to drug discovery (Figure 1G).

RESULTS AND DISCUSSION

Applying the reaction conditions of the previously developed ATRA of styrene (**A1**) and aroyl chlorides,[22] replacing the latter with ethyl chlorooxoacetate (**B1**, $E_{1/2}$ −1.18 V vs SCE) resulted in no formation of the desired product **1** (conditions A, Table 1, entry 1). This was unexpected given the favorable excited-state reduction potential and excited-state lifetime of the heteroleptic Cu(I) photocatalyst $[Cu(dmp)(BINAP)]BF_4$ ($E^*_{1/2} = -1.64$ V vs SCE; $\tau = 2188$ ns) employed, which should easily allow SET to **B1**. The failure of this mode of activation could have been due to the inability of **B1** to undergo heterolytic C−Cl bond cleavage to generate the active Cu(I)-Cl species (*cf.*

https://doi.org/10.1021/acscatal.6c03087
ACS Catal. XXXX, XXX, XXX−XXX

Table 1. Reaction Development[a,b]

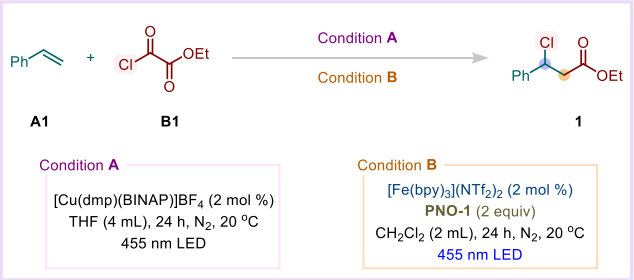

Entry	Deviation from condition A	Yield (%)[d]
1	None	0
2	2,6-lutidine / **PNO-6** (2 equiv.)	0
3	[Cu(phen)(XantPhos)]BF_4 + PNO-6	20
4	[Cu^I(dap)$_2$]Cl / [Cu^I(dmp)$_2$]Cl	0
Entry	**Deviation from condition B**	**Yield (%)[e]**
5	none	46
6	THF / Acetone / MeOH / $CHCl_3$	22 / 0/ 0/ 0
7	CH_2Cl_2 (1 mL / 0.5 mL)	54 / 60
8[b]	**PNO-1** (1 equiv.)	61
9[b,c]	**PNO-2 / PNO-3 / PNO-4 / PNO-5**	36/63/9/60
10[b,c]	**PNO-6**	85
11[b,c]	**PNO-7 / PNO-8**	46 / 0
12[b,d]	[Fe(dtbbpy)$_3$](NTf$_2$)$_2$	48
13[b,d]	2.0 mol % Fe(OAc)$_2$	47
14[b,d]	Without [Fe(bpy)$_3$](NTf$_2$)$_2$	Trace
15[b,d]	**0.5 mol % [Fe(bpy)$_3$](NTf$_2$)$_2$**	**85(83)**[f]
16[b]	2,6-lutidine (1 equiv.) instead of **PNO-6**	0
17[b,d]	no light	0
18[b,d]	Under air	47

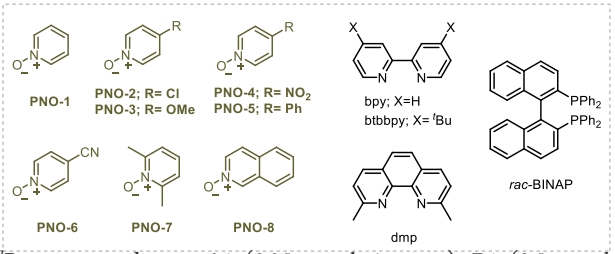

[a]Reaction conditions: **A1** (0.25 mmol, 1 equiv.), **B1** (0.5 mmol, 2 equiv.), [Fe(bpy)$_3$](NTf$_2$)$_2$ (2 mol %), **PNO-1** (2 equiv.), CH_2Cl_2 (2.0 mL, 0.125 M), under N_2, 20 °C, 24 h, 455 nm light irradiation. [b]CH_2Cl_2 (0.5 mL, 0.5 M). [c]**PNO** (1 equiv.). [d]**PNO-6** (1 equiv.). [e]The ^{1}H-NMR yields were measured using 1,1,2,2-tetrachloroethane as the internal standard. [f]Yield of the isolated product.

Scheme 1B). 2,6-Lutidine or 4-cyanopyridine *N*-oxide (**PNO-6**) as additives were ineffective (Table 1, entry 2). Other heteroleptic Cu(I) photocatalysts screened did not show a significant improvement: Best results were achieved with [Cu(phen)(XantPhos)]BF_4 ($E^*_{1/2}$ = −1.69 V vs SCE, τ = 391 ns) in combination with **PNO-6**, giving rise to product **1** in nevertheless low yield (20%, Table 1, entry 3; for details, see the Supporting Information (SI)). Well-established homoleptic Cu(I)-based photocatalysts such as [Cu^I(dap)$_2$]Cl (dap = 2,9-di(*p*-anisyl-1,10-phenanthroline)); ($E^*_{1/2}$ = −1.43 V vs SCE, τ = 270 ns) and [Cu^I(dmp)$_2$]Cl (dmp = 2,9- di(*p*-anisyl-1,10- phenanthroline)); ($E^*_{1/2}$ = −1.54 V vs SCE, τ = 90 ns) were also unsuccessful (Table 1, entry 4; for details, see the Supporting Information). Unexpectedly, the ultrashort excited-state lifetime of the iron-bipyridine complex (MLCT state, $E^*_{1/2}$ unavailable, τ <200 fs; $^5T_2$ state, $E^*_{1/2}$ ca. –0.09 V vs SCE;[39] τ = 1 ns[39−41]), in combination with pyridine-*N*-oxide, gave rise to the desired product **1** in 46% yield (condition B, Table 1, entry 5). The choice and concentration of solvent and pyridine *N*-oxide additive are critical for the reaction outcome: CH_2Cl_2 at a concentration of 0.5 M (Table 1, entries 5−7) and 4-cyanopyridine *N*-oxide, **PNO-6** (Table 1, entries 8−11; for details, see the Supporting Information) resulted in further improvements, giving rise to **1** in 83% isolated yield at a low loading of [Fe(bpy)$_3$](NTf$_2$)$_2$ (0.5 mol %; entry 15). Other Fe(II)-bipyridine/phenanthroline complexes[37] such as [Fe(dtbbpy)$_3$](NTf$_2$)$_2$, [Fe(phen)$_3$](NTf$_2$)$_2$, or [Fe(Me$_4$phen)$_3$](NTf$_2$)$_2$ gave inferior results (Table 1, entry 12; for details, see the Supporting Information). Notably, a control experiment with simple iron salts, e.g., Fe(OAc)$_2$ at a higher catalyst loading (2 mol %), also produced the desired product, albeit with lower yield (47%, Table 1, entry 13; for details, see the Supporting Information). The presence of iron is vital for the reaction (Table 1, entry 14). The use of 2,6-lutidine as an additive, successful in the presence of Ru/Ir-based photocatalysts (*cf.* Figure 1F),[28] proved ineffective (entry 16). The indispensability of light irradiation and an inert atmosphere in the process was confirmed by performing background experiments in the dark and under air, respectively (entries 17 and 18).

Having optimized the reaction conditions, we next explored the scope by employing a broad range of activated and unactivated alkenes (Scheme 1). Electronically diverse para-substituents surveyed on the arene moiety in the styrene partner included methyl, phenyl, fluoro, chloro, nitro, trifluoromethyl, acetoxy, carboxyl acid, methyl ester, chloromethylene, and trimethylsilyl gave the desired products **2**−**12** (52–83% yield). We further examined positional bias on the arene moiety: meta- and ortho-substituted vinyl arenes showed high competency in this transformation (**13**−**15**, 70−88% yield). Inclusion of strong +M groups (e.g., *p*-OMe and *p*-O^{t}Bu) on the styrene partner led to the formation of corresponding dehydrochlorinated α,β-unsaturated esters (**16**−**18**), whereas sterically crowded 2,4,6-trimethyl styrene gave the mixture of ATRA as well as dehydrochlorinated product **19**. This might be an indication for a diversion in the mechanism, i.e., for these substrates, the oxidation of the radical intermediate of type **V** to the cation **VI** proceeds as opposed to deliver the chlorine via an Fe(III)-Cl species **b** (*cf.* mechanistic discussion, *vide infra* Figure 2E). Vinyl arene derivatives adorned with a substituent flanking at the α- or β-position of the double bond are suitable substrates as well, giving rise to the desired products **20** and **21**. β-Chloroesterification of indene provided **22** as a diastereomeric mixture. Polyaromatic and heteroaromatic styrene analogues were also successfully assessed, bearing naphthyl and thiazolyl *in lieu* of a benzenoid ring (**23** and **24**).

Various unactivated alkenes were viable substrates for the title reaction as well (Scheme 1B). An extension of the reaction

https://doi.org/10.1021/acscatal.6c03087
ACS Catal. XXXX, XXX, XXX−XXX

Scheme 1. Substrate Scope of Alkoxycarbonylchlorination of Alkenes[c]

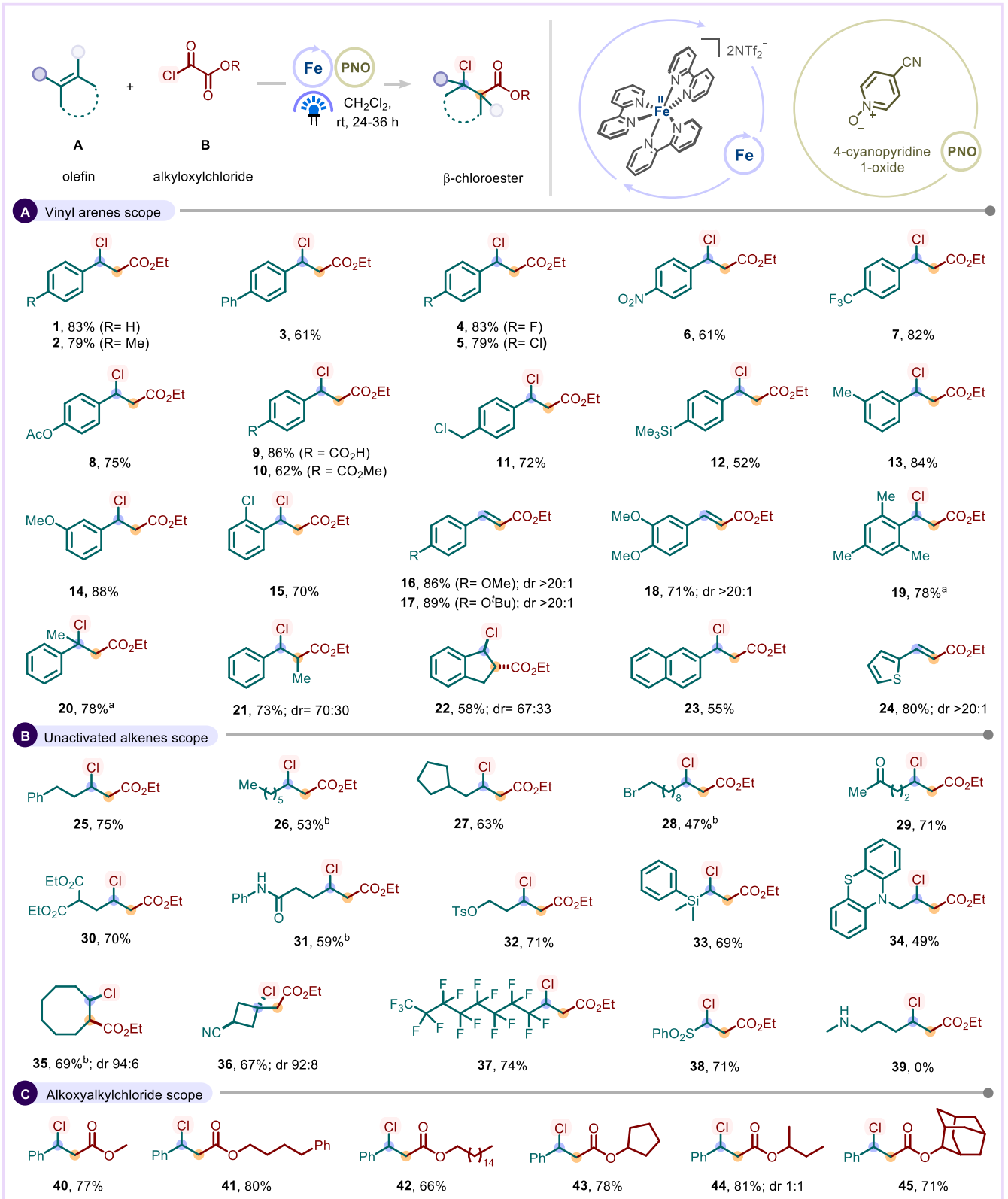

[a]Compounds are obtained as a mixture of ATRA and dehydrochlorination products.[b]Compounds are obtained with the mixture of corresponding alkyl ethyl oxalate derivatives as the side products due to competitive addition of **III** to the alkenes; yields are of the isolated products.[c](A) Vinyl arene scope. (B) Unactivated alkene scope. (C) Alkoxyalkyl chloride scope. Reaction conditions: (for activated alkenes) **A** (0.25 mmol, 1 equiv.), **B** (0.5 mmol, 2 equiv.), $[Fe(bpy)_3](NTf_2)_2$ (0.5 mol %), 4-cyanopyridine 1-oxide (1 equiv.), CH_2Cl_2 (0.5 mL, 0.5 M), under N_2, 20 °C, 24 h, 455 nm light irradiation; (for unactivated alkenes) **A** (0.5 mmol, 2 equiv.), **B** (0.25 mmol, 1 equiv.), $[Fe(bpy)_3](NTf_2)_2$ (0.5 mol %), 4-cyanopyridine 1-oxide (1 equiv.), CH_2Cl_2 (0.5 mL, 0.5 M), under N_2, 20 °C, 36 h, 455 nm light irradiation.

https://doi.org/10.1021/acscatal.6c03087
ACS Catal. XXXX, XXX, XXX−XXX

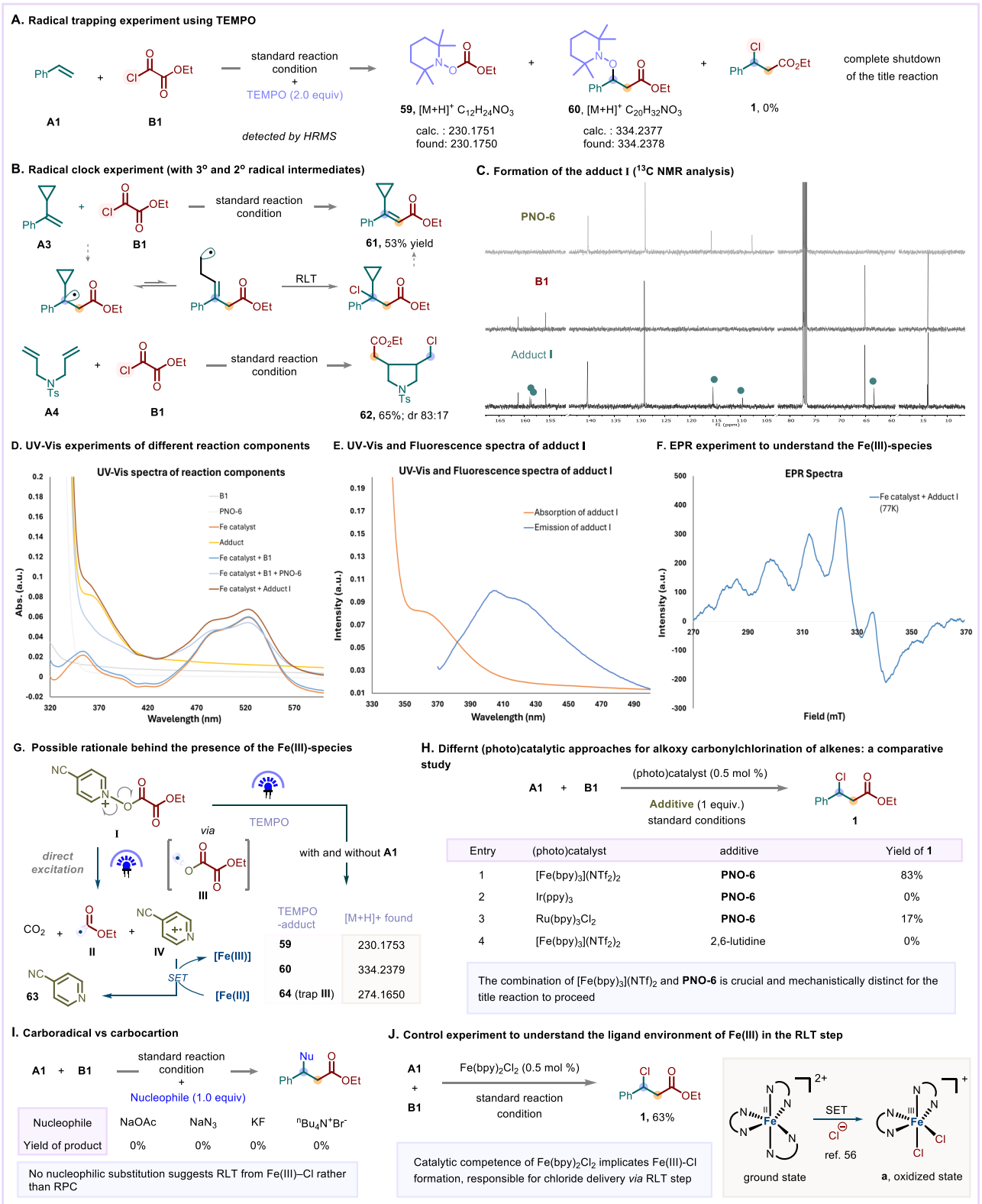

Figure 2. Detailed mechanistic studies. (A) Radical trapping experiment. (B) Radical clock experiment. (C) NMR analysis for the formation of the adduct **I**.(D) UV−visible studies of different reaction components and their combinations. (E) UV−visible and fluorescence studies of the adduct **I** to confirm its photoactive nature. (F) Electronic paramagnetic resonance (EPR) studies to confirm the presence of Fe(III) species. (G) Irradiation of **I** without iron complex. (H) Comparative photochemical study of the title reaction using different (photo)catalysts along with iron. (I) Study of the title reaction in the presence of an external nucleophile. (J) Control experiment performing the title reaction with $Fe(bpy)_2Cl_2$ to understand the ligand environment around Fe(III) in the RLT step.

https://doi.org/10.1021/acscatal.6c03087
ACS Catal. XXXX, XXX, XXX−XXX

time to 36 h was necessary in order to obtain **25**−**34** in good yields, further underscoring the functional group (e.g., halide, ketone, ester, amide, tosyl, and silyl) tolerance of this chloroesterification protocol. Alkenes bearing endocyclic (**35**) and exocyclic double bonds (**36**) furnished the desired products with excellent regio- and appreciable stereoselectivity. Moreover, highly electron-deficient perfluorodecene and the Michael acceptor phenyl vinyl sulfone afforded the corresponding β-chloroesters **37** and **38** with 74 and 71% yields, respectively. The limitation was found for an amino group present in the alkene due to direct coupling with the acid chloride used (**39**).

Variation of the alkoxyalyl chlorides was also possible. Commercially available methyl oxalyl chloride as well as the alkoxycarbonyl radical precursors derived from phenyl-1- butanol and cetyl alcohol were found to be successful in the title transformation (**40**−**42**) as were secondary alkyloxyalyl chlorides derived from carbocyclic cyclopentyl alcohol, branched 2-butanol, and sterically demanding congested 1-adamentol (**43**−**45**).

We next explored the late-stage modifications of biologically relevant scaffolds by anchoring pharmaceuticals and natural products such as ibuprofen, naproxen, theophylline, Vit-E, fenofibrate, with suitable vinyl arenes (**46**−**50**, Scheme 2, 86−68% yield). Furthermore, unactivated alkenes derived from methyl paraben, Vit-E, oxaprozin, indomethacine, estrone, and caryophyllene were converted into the corresponding β-chloroesters in good yields (**51**−**56**, 69−51% yield). Finally, alkoxyalyl chloride

Scheme 2. Substrate Scope of Late-Stage Alkoxycarbonyl Chlorination of Alkenes[a]

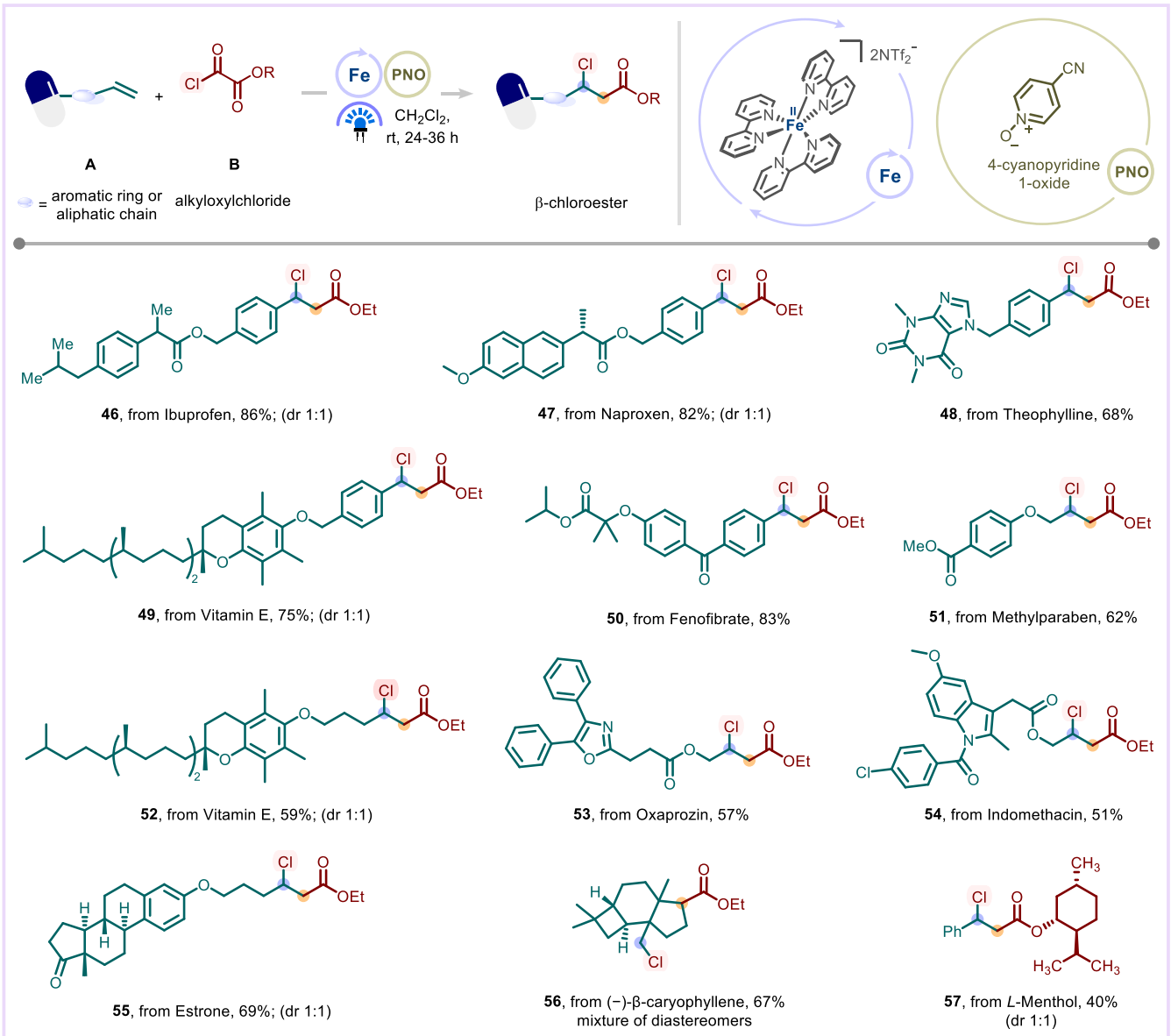

[a]Reaction conditions: (for activated alkenes) **A** (0.25 mmol, 1 equiv.), **B** (0.5 mmol, 2 equiv.), $[Fe(bpy)_3](NTf_2)_2$ (0.5 mol %), 4-cyanopyridine 1-oxide (1 equiv.), CH_2Cl_2 (0.5 mL, 0.5 M), under N_2, 20 °C, 24 h, 455 nm light irradiation; (for unactivated alkenes) **A** (0.5 mmol, 2 equiv.), **B** (0.25 mmol, 1 equiv.), $[Fe(bpy)_3](NTf_2)_2$ (0.5 mol %), 4-cyanopyridine 1-oxide (1 equiv.), CH_2Cl_2 (0.5 mL, 0.5 M), under N_2, 20 °C, 36 h, 455 nm light irradiation; yields are of the isolated products.

https://doi.org/10.1021/acscatal.6c03087
ACS Catal. XXXX, XXX, XXX−XXX

derived from chiral L-menthol furnished the desired product **57** with 40% yield.

Alkynes showed no conversion in the title reaction, which can be turned into an advantage by selectively converting a double bond in the presence of a triple bond as demonstrated with product **58** (Scheme 3A). 4-Vinyl pyridine was not amenable with the process, presumably due to either coordination of this substrate to Fe(III) or reaction with **B1**, forming an acylpyridinium salt.[28] Moreover, vinyl ethers could also not be engaged in the title reaction, suggesting a philicity-mismatched radical addition of nucleophilic radical **II** to such alkenes (*vide infra, mechanistic discussion*).

Scale-up was demonstrated by using styrene (**A1**, 5 mmol) and ethyloxochloroacetate (**B1**) to give rise to the corresponding β-chloroester **1** in 78% yield (Scheme 3B).

Mechanistic studies were conducted to probe the radical nature of the process (Figure 2). Addition of 2,2,6,6-tetramethylpiperidine-1-oxyl (TEMPO) completely inhibited the reaction, and the TEMPO adducts of the possible radical intermediates **59** and **60** were detected by HRMS analysis, supporting the formation of corresponding radical intermediates **II** and **V**, respectively. A radical clock reaction with 1-cyclopropylstyrene **A3** afforded the product **61** in 53% yield, which suggests that the corresponding tertiary benzylic radical is the decisive intermediate.[42] When *N*-tosyldiallyl amine **A4** was employed as a radical clock partner, the cyclized product **62** was formed (65% yield, 83:17 dr), further supporting the radical pathway. The low quantum yield ($\Phi = 0.047$) determined for the reaction between **A1** and **B1** indicates that a radical chain manifold is either very unlikely or highly unproductive (for details, see the Supporting Information).

The presence of 4-cyanopyridine *N*-oxide **PNO-6** is essential for the success of the reaction, which can be understood with the facile formation of adduct **I** that was confirmed by ^{1}H and ^{13}C NMR analyses (Figure 2C; for details, see the Supporting Information). UV−vis studies showed absorption of $[Fe(bpy)_3](NTf_2)_2$ in the visible region, but no absorption of the reactants **B1** and **PNO-6** (Figure 2D). The UV−vis experiment further evidenced that **I** has a strong absorption near 370 nm that extends beyond 400 nm, while fluorescence measurements showed a significant emission, indicating its photoactive nature under the reaction conditions (Figure 2E). When $[Fe(bpy)_3](NTf_2)_2$ was added to **I**, there was no shift in the absorption maxima, which implies no interaction of the Fe complex with adduct **I** in the excited state (Figure 2D). In agreement with the very short excited-state lifetime of $[Fe(bpy)_3]^{2+}$ (MLCT state, $E^*_{1/2}$ unavailable, τ <200 fs; $^5T_2$ state, $E^*_{1/2}$ ca. –0.09 V vs SCE;[39] τ = 1 ns[39−41]), as further evidenced by the photophysical investigations by McCusker et al. and others,[39,40,43−50] and its insufficient excited-state redox potential, we consider therefore a photoinduced SET from the iron(II)bpy complex ($E^*_{1/2}$ = ca. –0.09 V vs SCE[39]) to **I** ($E_{1/2}$ –1.17 V vs SCE) to be unlikely. However, analysis by electron paramagnetic resonance (EPR) of a mixture of $[Fe(bpy)_3](NTf_2)_2$ and adduct **I** upon visible-light irradiation confirmed the presence of a Fe(III) species (Figure 2F). We therefore propose that the ground-state SET process between Fe(II) ($E_{1/2}$ = ca. 1.03 V vs SCE[39]) and pyridinium radical cation intermediate **IV** arising from the direct photoinduced N−O bond fragmentation of **I** (Figure 2G) occurs. Further evidence for the direct excitation of **I** followed by homolysis was obtained by probing the corresponding radical intermediates **II** and **III**: When **I** was solely irradiated with TEMPO, the adducts **59** and **64**, respectively, were detected by MS spectrometry (Figure 2G).

Moreover, a comparative study of different photocatalytic approaches for the title ATRA transformation was executed (Figure 2H). In our developed reaction conditions, usage of traditional Ir(III)- or Ru(II)-based photocatalysts replacing the Fe(II) catalyst showed a detrimental effect: Ir(III) yielded no desired ATRA product **1**, whereas Ru(II) afforded only 17% yield of **1**, thereby showcasing their incompatibility for this process (Figure 2H, entries 2 and 3). On the other hand, $[Fe(bpy)_3](NTf_2)_2$ failed to provide **1** in the presence of 2,6-lutidine as an additive instead of **PNO-6**, indicating the inability of $[Fe(bpy)_3](NTf_2)_2$ to act as a photocatalyst to perform the SET of a 2,6-lutidine/**B1** adduct (Figure 2H, entry 4). These results highlight the crucial role of $[Fe(bpy)_3](NTf_2)_2$ as the e^--shuttle catalyst in combination with pyridine *N*-oxide as the activator of **B1** for the success of the title reaction, thereby distinguishing the mechanism of our protocol from previous studies.[28]

On the basis of the above experimental results along with the control experiments (*cf.* Table 1, entry 13) and previous reports by Stephenson, West, Katayev, Bao, and others,[24−27,29−38] a plausible mechanism is proposed in Figure 3. *In situ* generated adduct **I** gets excited upon visible-light irradiation, which triggers the photolytic fragmentation of the N−O bond to alkoxyl radical **III** and pyridinyl radical cation **IV**. **III** subsequently undergoes decarboxylation to generate acyl radical **II** followed by addition to the alkene, forming the radical **V**. On the other hand, $[Fe(bpy)_3]^{2+}$ reduces **IV** to 4-cyanopyridine (**63**), which was confirmed by ^{1}H-NMR analysis of the reaction mixture and can easily be recovered following chromatographic purification (for details, see the Supporting Information). To understand the probable architecture of the Fe(III) intermediate, a control experiment was done using $Fe^{II}(bpy)_2Cl_2$[51,52] instead of $Fe(bpy)_3(NTf_2)_2$ (Figure 2J) giving ATRA product **1** 63% yield. Since $Fe(bpy)_3^{2+}$ is photostable[39,43−46] even in the presence of chloride (see the Supporting Information for details), $Fe^{II}(bpy)_2Cl_2$ cannot be formed by ligand exchange. However, after oxidation to $[Fe^{III}(bpy)_3]^{3+}$,[53−55] ligand exchange with chloride to form $[Fe^{III}(bpy)_2Cl_2]^+$ (**a**) must be facile in line with literature reports.[56−58] We therefore propose that a Fe(III)-Cl

Scheme 3. (A) Chemoselectivity Experiment and (B) Scale-up Experiment

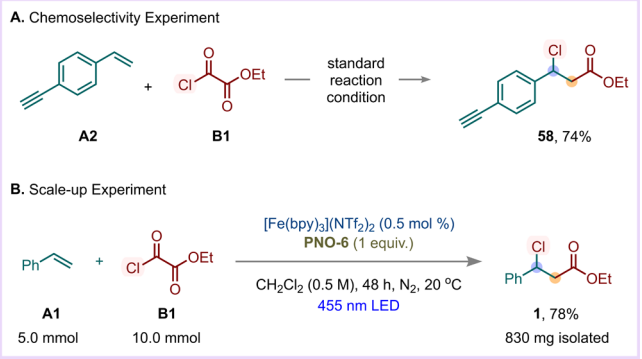

https://doi.org/10.1021/acscatal.6c03087
ACS Catal. XXXX, XXX, XXX−XXX

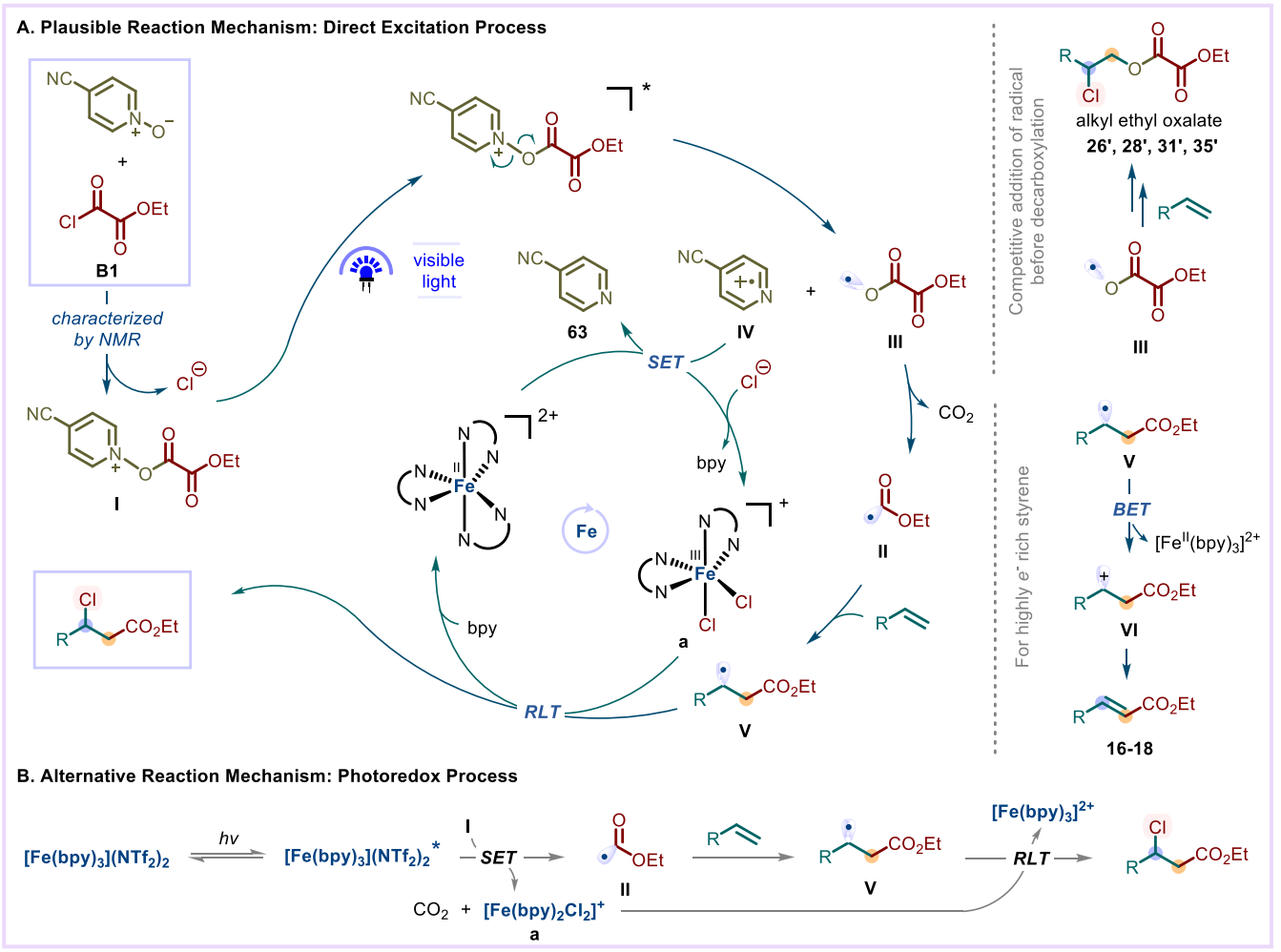

Figure 3. Photocatalytic cycles for the alkoxycarbonylchlorination of alkenes. (A) Plausible reaction mechanism considering the direct excitation of **I**. (B) Alternative reaction mechanism considering Fe(II) as the photoredox catalyst.

intermediate such as **a** transfers a chlorine atom to **V** via RLT, thereby delivering the desired ATRA product.

To validate our hypothesis on the Cl delivery via the RLT process, we explored the plausibility of the oxidation of carboradical **V** to carbocation **VI**. When the title reaction was performed in the presence of different nucleophiles (OAc^-, N_3^-, F^-, and Br^-), no nucleophilic addition product has been detected (Figure 2F), although the ATRA product **1** was achieved in considerable yields (see the Supporting Information for details). This result makes a radical-polar crossover (RPC) pathway unlikely and supports the proposal that chloride is being delivered via an RLT event from Fe^{III}–Cl species **a**. Only for styrene derivatives bearing strongly electron-donating substituents, the reaction appears to proceed via an RPC mechanism by oxidation of the radical intermediate **V** to the corresponding carbocation **VI** followed by deprotonation (Figure 3), as seen in the formation of **16**–**18**.

The competitive addition of **III** to the alkenes before decarboxylation could also be possible, which yielded corresponding alkyl ethyl oxalate derivatives **26′**, **28′**, **31′**, and **35′** as the side products with **26**, **28**, **31**, and **35**, respectively (for details, see Figure 3 and Supporting Information). This further supports the formation of **III** as a reactive radical intermediate, arising from the photofragmentation of the N–O bond of **I** (Figure 3A), rather than by the photoinduced SET reduction of $[Fe(bpy)_3](NTf_2)_2$ (Figure 3B), which was reported to be possible for the reduction of α-bromocarbonyl compounds in the asymmetric alkylation of aldehydes by Cozzi et al.[38]

■ CONCLUSIONS

Alkyloxalyl chlorides, generated *in situ* from the corresponding alcohols and oxalyl chloride, can be exploited as ATRA reagents under visible-light photoredox catalysis for olefin difunctionalization. In this approach, we have realized a Fe(II)-catalyzed alkoxycarbonylchlorination of alkenes in combination with 4-cyanopyridine-*N*-oxide, used as an activator for alkyloxalyl chlorides. The title transformation features mild reaction conditions, good functional group tolerance, and operational simplicity. An array of activated and unactivated alkenes was functionalized in a highly regio- and chemoselective manner, which permits access to the corresponding saturated and unsaturated aliphatic esters. The synthetic utility has been further demonstrated through the expedited synthesis of β-chloroesters derived from alkenes containing bioactive molecules. Mechanistic studies suggest the decarboxylative N–O bond fragmentation of a photocleavable alkyloxalyl chloride-pyridine-*N*-oxide adduct by direct excitation in combination with radical ligand transfer (RLT) of chlorine, for which Fe(III)-Cl species, generated *in situ* in a catalytic fashion, are key intermediates. The strategy delineated here will provide a

https://doi.org/10.1021/acscatal.6c03087
ACS Catal. XXXX, XXX, XXX–XXX

set of tools for activating different Csp^2-X precursors to incorporate acyl and halogen functionalities across a double bond, obviating the need for precious Ir/Ru photocatalysts, and will spur the development of photochemical ATRA methods that proceed via a ligand transfer pathway utilizing inexpensive Fe(II)-bipyridine complexes.

METHODS

General Procedure A

To a glass reaction vial (5 mL size) equipped with a stir bar $[Fe(bpy)_3](NTf_2)_2$ (1.5 mg, 0.00125 mmol), 4-cyanopyridine 1-oxide **PNO-6** (30.0 mg, 0.25 mmol), vinyl arene **A** (if solid at room temperature, 0.25 mmol), and alkyl chlorooxoacetate **B** (if solid at room temperature, 0.5 mmol) were added. The vial was then sealed with a crimp-cap and evacuated-backfilled with N_2 thrice. CH_2Cl_2 (0.5 mL) was added, and the solution was purged with nitrogen for 2−3 min. Then, vinyl arene **A** (if liquid at room temperature, 0.25 mmol) and alkyl chlorooxoacetate **B** (if liquid at room temperature, 0.5 mmol) were added to the solution under positive nitrogen atmosphere. The vial was irradiated with blue LED (λ_{max} 455 nm) at room temperature for 24 h. After completion of the reaction (monitored by TLC analysis), the reaction mixture was diluted with CH_2Cl_2 and transferred to a round-bottom flask. Following concentration in vacuo, the crude product was purified by column chromatography on silica (eluent: hexanes and ethyl acetate in the ratio indicated in the individual procedures).

General Procedure B

To a glass reaction vial (5 mL size) equipped with a stir bar $[Fe(bpy)_3](NTf_2)_2$ (1.5 mg, 0.00125 mmol), 4-cyanopyridine 1-oxide PNO-6 (30.0 mg, 0.25 mmol), unactivated alkene A (if solid at room temperature, 0.5 mmol), and alkyl chlorooxoacetate B (if solid at room temperature, 0.25 mmol) were added. The vial was then sealed with a crimp-cap and evacuated-backfilled with N_2 thrice. CH_2Cl_2 (0.5 mL) was added, and the solution was purged with nitrogen for 2−3 min. Then, unactivated alkene A (if liquid at room temperature, 0.5 mmol) and alkyl chlorooxoacetate B (if liquid at room temperature, 0.25 mmol) were added to the solution under a positive nitrogen atmosphere. The vial was irradiated with blue LED (λ_{max} 455 nm) at room temperature for 36 h. After completion of the reaction (monitored by TLC analysis), the reaction mixture was diluted with CH_2Cl_2 and transferred to a round-bottom flask. Following concentration in vacuo, the crude product was purified by column chromatography on silica (eluent: hexanes and ethyl acetate in the ratio indicated in the individual procedures).

ASSOCIATED CONTENT

Data Availability Statement

The data underlying this study are available in the published article and its Supporting Information. The primary research data of this study are openly available in Radar4Chem at DOI: 10.22000/dpb0bd790dm0vysx.

Supporting Information

The Supporting Information is available free of charge at https://pubs.acs.org/doi/10.1021/acscatal.6c03087.

Detailed experimental procedures, materials, and methods, including photographs of the experimental setup, details of mechanistic studies, compound characterizations, and ^1H, ^{13}C NMR, and ^{19}F spectra of all isolated compounds. (PDF)

AUTHOR INFORMATION

Corresponding Author

Oliver Reiser – *Institut für Organische Chemie, Universität Regensburg, Universitätsstrasse 31, Regensburg 93053, Germany*; orcid.org/0000-0003-1430-573X; Email: oliver.reiser@chemie.uni-regensburg.de

Authors

Mangish Ghosh – *Institut für Organische Chemie, Universität Regensburg, Universitätsstrasse 31, Regensburg 93053, Germany*; orcid.org/0009-0005-2632-303X

Tirtha Mandal – *Institut für Organische Chemie, Universität Regensburg, Universitätsstrasse 31, Regensburg 93053, Germany*; orcid.org/0000-0003-0487-0268

Zen Shimizu – *Institut für Organische Chemie, Universität Regensburg, Universitätsstrasse 31, Regensburg 93053, Germany*

Complete contact information is available at: https://pubs.acs.org/doi/10.1021/acscatal.6c03087

Author Contributions

[§]M.G. and T.M. contributed equally to this work.

Notes

The authors declare no competing financial interest.

ACKNOWLEDGEMENT

This work was supported by the Deutsche Forschungsgemeinschaft (DFG, German Research Foundation) − TRR 325444632635-A1.

REFERENCES

(1) Kharasch, M. S.; Urry, W. H.; Jensen, E. V. Addition of derivatives of chlorinated acetic acids to olefins. *J. Am. Chem. Soc.* **1945**, *67*, No. 1626.

(2) Kharasch, M. S.; JENSEN, E. V.; Urry, W. H. Addition of carbon tetrachloride and chloroform to olefins. *Science* **1945**, *102*, 128.

(3) Barton, D. H.; Csiba, M. A.; Jaszberenyi, J. C. $Ru(bpy)_3^{2+}$-mediated addition of Se-phenyl p-tolueneselenosulfonate to electron rich olefins. *Tetrahedron Lett.* **1994**, *35*, 2869–2872.

(4) Wallentin, C.-J.; Nguyen, J. D.; Finkbeiner, P.; Stephenson, C. R. J. Visible light-mediated atom transfer radical addition via oxidative and reductive quenching of photocatalysts. *J. Am. Chem. Soc.* **2012**, *134*, 8875–8884.

(5) Courant, T.; Masson, G. Recent Progress in Visible-Light Photoredox-Catalyzed Intermolecular 1,2-Difunctionalization of Double Bonds via an ATRA-Type Mechanism. *J. Org. Chem.* **2016**, *81*, 6945–6952.

(6) Stephenson, C. R.; Yoon, T. P.; MacMillan, D. W. *Visible Light Photocatalysis in Organic Chemistry*; John Wiley & Sons, **2018**.

(7) Voutyritsa, E.; Triandafillidi, I.; Kokotos, C. G. Expanding the Scope of Photocatalysis: Atom Transfer Radical Addition of Bromoacetonitrile to Aliphatic Olefins. *ChemCatChem* **2018**, *10*, 2466–2470.

(8) Klauck, F. J. R.; Yoon, H.; James, M. J.; Lautens, M.; Glorius, F. Visible-Light-Mediated Deaminative Three-Component Dicarbofunctionalization of Styrenes with Benzylic Radicals. *ACS Catal.* **2019**, *9*, 236–241.

(9) Wang, H.; Gao, Y.; Zhou, C.; Li, G. Visible-Light-Driven Reductive Carboarylation of Styrenes with CO_2 and Aryl Halides. *J. Am. Chem. Soc.* **2020**, *142*, 8122–8129.

(10) Kosobokov, M. D.; Zubkov, M. O.; Levin, V. V.; Kokorekin, V. A.; Dilman, A. D. Fluoroalkyl sulfides as photoredox-active coupling reagents for alkene difunctionalization. *Chem. Commun.* **2020**, *56*, 9453–9456.

(11) Reiser, O. Shining Light on Copper: Unique Opportunities for Visible-Light-Catalyzed Atom Transfer Radical Addition Reactions and Related Processes. *Acc. Chem. Res.* **2016**, *49*, 1990–1996.

(12) Hossain, A.; Bhattacharyya, A.; Reiser, O. Copper's rapid ascent in visible-light photoredox catalysis. *Science* **2019**, *364*, No. eaav9713.
(13) Engl, S.; Reiser, O. Copper-photocatalyzed ATRA reactions: concepts, applications, and opportunities. *Chem. Soc. Rev.* **2022**, *51*, 5287–5299.
(14) Zhong, M.; Pannecoucke, X.; Jubault, P.; Poisson, T. Recent advances in photocatalyzed reactions using well-defined copper(I) complexes. *Beilstein J. Org. Chem.* **2020**, *16*, 451–481.
(15) Rawner, T.; Lutsker, E.; Kaiser, C. A.; Reiser, O. The Different Faces of Photoredox Catalysts: Visible-Light-Mediated Atom Transfer Radical Addition (ATRA) Reactions of Perfluoroalkyl Iodides with Styrenes and Phenylacetylenes. *ACS Catal.* **2018**, *8*, 3950–3956.
(16) Engl, S.; Reiser, O. Copper Makes the Difference: Visible Light-Mediated Atom Transfer Radical Addition Reactions of Iodoform with Olefins. *ACS Catal.* **2020**, *10*, 9899–9906.
(17) Reichle, A.; Koch, M.; Sterzel, H.; Großkopf, L.-J.; Floss, J.; Rehbein, J.; Reiser, O. Copper(I) Photocatalyzed Bromonitroalkylation of Olefins: Evidence for Highly Efficient Inner-Sphere Pathways. *Angew. Chem., Int. Ed.* **2023**, *62*, No. e202219086.
(18) Abderrazak, Y.; Reiser, O. Copper Photocatalyzed Divergent Access to Organic Thio- and Isothiocyanates. *ACS Catal.* **2024**, *14*, 4847–4855.
(19) Lei, Z.; Banerjee, A.; Kusevska, E.; Rizzo, E.; Liu, P.; Ngai, M.-Y. β-Selective Aroylation of Activated Alkenes by Photoredox Catalysis. *Angew. Chem., Int. Ed.* **2019**, *58*, 7318–7323.
(20) Patil, D. V.; Kim, H. Y.; Oh, K. Visible Light-Promoted Friedel-Crafts-Type Chloroacylation of Alkenes to β-Chloroketones. *Org. Lett.* **2020**, *22*, 3018–3022.
(21) Zheng, M.; Hou, J.; Zhan, L.-W.; Huang, Y.; Chen, L.; Hua, L.-L.; Li, Y.; Tang, W.-Y.; Li, B.-D. Visible-Light-Driven, Metal-Free Divergent Difunctionalization of Alkenes Using Alkyl Formates. *ACS Catal.* **2021**, *11*, 542–553.
(22) Mandal, T.; Ghosh, M.; Paps, H.; Mandal, T.; Reiser, O. A general photocatalytic platform for the regio- and stereoselective β-chloroacylation of alkenes and alkynes using a heteroleptic copper(I) complex. *Nat. Catal.* **2025**, *8*, 607–622.
(23) Minozzi, C.; Caron, A.; Grenier-Petel, J.-C.; Santandrea, J.; Collins, S. K. Heteroleptic Copper(I)-Based Complexes for Photocatalysis: Combinatorial Assembly, Discovery, and Optimization. *Angew. Chem., Int. Ed.* **2018**, *57*, 5477–5481.
(24) Beatty, J. W.; Douglas, J. J.; Cole, K. P.; Stephenson, C. R. J. A scalable and operationally simple radical trifluoromethylation. *Nat. Commun.* **2015**, *6* , No. 7919.
(25) Beatty, J. W.; Douglas, J. J.; Miller, R.; McAtee, R. C.; Cole, K. P.; Stephenson, C. R. J. Photochemical Perfluoroalkylation with Pyridine N-Oxides: Mechanistic Insights and Performance on a Kilogram Scale. *Chem* **2016**, *1*, 456–472.
(26) McClain, E. J.; Wortman, A. K.; Stephenson, C. R. J. Radical generation enabled by photoinduced N-O bond fragmentation. *Chem. Sci.* **2022**, *13*, 12158–12163.
(27) McClain, E. J.; Monos, T. M.; Mori, M.; Beatty, J. W.; Stephenson, C. R. J. Design and Implementation of a Catalytic Electron Donor–Acceptor Complex Platform for Radical Trifluoromethylation and Alkylation. *ACS Catal.* **2020**, *10*, 12636–12641.
(28) Chen, J.-Q.; Tu, X.; Tang, Q.; Li, K.; Xu, L.; Wang, S.; Ji, M.; Li, Z.; Wu, J. Efficient access to aliphatic esters by photocatalyzed alkoxycarbonylation of alkenes with alkyloxalyl chlorides. *Nat. Commun.* **2021**, *12*, No. 5328.
(29) Bian, K.-J.; Kao, S.-C.; Nemoto, D.; Chen, X.-W.; West, J. G. Photochemical diazidation of alkenes enabled by ligand-to-metal charge transfer and radical ligand transfer. *Nat. Commun.* **2022**, *13*, No. 7881.
(30) Bian, K.-J.; Yu, S.; Chen, Y.; Liu, Q.; Chen, X.; Nemoto, D.; Kao, S.-C.; Martí, A. A.; West, J. G. Photocatalytic anti-Markovnikov hydro- and haloazidation of alkenes. *Nat. Commun.* **2025**, *16*, No. 7906.
(31) Bian, K.-J.; Nemoto, D.; Chen, X.-W.; Kao, S.-C.; Hooson, J.; West, J. G. Photocatalytic, modular difunctionalization of alkenes enabled by ligand-to-metal charge transfer and radical ligand transfer. *Chem. Sci.* **2023**, *15*, 124–133.
(32) Ge, L.; Zhou, H.; Chiou, M.-F.; Jiang, H.; Jian, W.; Ye, C.; Li, X.; Zhu, X.; Xiong, H.; Li, Y.; Song, L.; Zhang, X.; Bao, H. Iron-catalysed asymmetric carboazidation of styrenes. *Nat. Catal.* **2021**, *4*, 28–35.
(33) Fernandes, A. J.; Katayev, D. Bimolecular Homolytic Substitution (S_H2) and Radical Ligand Transfer (RLT): Emerging Paradigms in Radical Transformations. *ACS Cent. Sci.* **2025**, *11*, 1812–1827.
(34) Patra, S.; Valsamidou, V.; Nandasana, B. N.; Katayev, D. Merging Iron-Mediated Radical Ligand Transfer (RLT) Catalysis and Mechanochemistry for Facile Dihalogenation of Alkenes. *ACS Catal.* **2024**, *14*, 13747–13758.
(35) Patra, S.; Mosiagin, I.; Giri, R.; Nauser, T.; Katayev, D. Electron-Driven Nitration of Unsaturated Hydrocarbons. *Angew. Chem., Int. Ed.* **2023**, *62*, No. e202300533.
(36) Gogoi, A. R.; Rentería-Gómez, Á.; Tan, T.-D.; Ng, J. W.; Koh, M. J.; Gutierrez, O. Iron-catalysed radical difunctionalization of alkenes. *Nat. Synth.* **2025**, *4*, 1036–1055.
(37) Parisien-Collette, S.; Hernandez-Perez, A. C.; Collins, S. K. Photochemical Synthesis of Carbazoles Using an $Fe(phen)_3(NTf_2)_2$/O_2 Catalyst System: Catalysis toward Sustainability. *Org. Lett.* **2016**, *18*, 4994–4997.
(38) Gualandi, A.; Marchini, M.; Mengozzi, L.; Natali, M.; Lucarini, M.; Ceroni, P.; Cozzi, P. G. Organocatalytic Enantioselective Alkylation of Aldehydes with $[Fe(bpy)_3]Br_2$ Catalyst and Visible Light. *ACS Catal.* **2015**, *5*, 5927–5931.
(39) Bowers, B. E.; Pfund, B.; Beissel, H. F.; Ghosh, A.; McCusker, J. K. Spin-State and Reorganization Energy Considerations for Metal-Centered Photoredox Catalysis. *J. Am. Chem. Soc.* **2025**, *147*, 39898–39911.
(40) Auböck, G.; Chergui, M. Sub-50-fs photoinduced spin crossover in $Fe(bpy)_3^{2+}$. *Nat. Chem.* **2015**, *7*, 629–633.
(41) de Groot, L. H. M.; Ilic, A.; Schwarz, J.; Wärnmark, K. Iron Photoredox Catalysis-Past, Present, and Future. *J. Am. Chem. Soc.* **2023**, *145*, 9369–9388.
(42) Newcomb, M. *Radical Kinetics and Clocks; Encyclopedia of Radicals in Chemistry, Biology and Materials*; John Wiley & Sons, Ltd, **2012**.
(43) Paulus, B. C.; Nielsen, K. C.; Tichnell, C. R.; Carey, M. C.; McCusker, J. K. A Modular Approach to Light Capture and Synthetic Tuning of the Excited-State Properties of Fe(II)-Based Chromophores. *J. Am. Chem. Soc.* **2021**, *143*, 8086–8098.
(44) Lee, A.; Son, M.; Deegbey, M.; Woodhouse, M. D.; Hart, S. M.; Beissel, H. F.; Cesana, P. T.; Jakubikova, E.; McCusker, J. K.; Schlau-Cohen, G. S. Observation of parallel intersystem crossing and charge transfer-state dynamics in Fe(bpy)32+ from ultrafast 2D electronic spectroscopy. *Chem. Sci.* **2023**, *14*, 13140–13150.
(45) Gawelda, W.; Cannizzo, A.; Pham, V.-T.; Mourik, F.van; Bressler, C.; Chergui, M. Ultrafast nonadiabatic dynamics of Fe(II)(bpy)(3)(2+) in solution. *J. Am. Chem. Soc.* **2007**, *129*, 8199–8206.
(46) McCusker, J. K. Electronic structure in the transition metal block and its implications for light harvesting. *Science* **2019**, *363*, 484–488.
(47) Magar, R. T.; Fortunato, M. T.; Curtin, G. M.; Deegbey, M.; Romero, M.; Maez, S. G.; Jakubikova, E.; Turro, C.; Rack, J. J. Kinetic trapping for the production of a long-lived 3MLCT excited state n Fe(II) complexes. *Chem. Commun.* **2025**, *61*, 19489–19492.
(48) Curtin, G. M.; Jakubikova, E. Extended π-Conjugated Ligands Tune Excited-State Energies of Iron(II) Polypyridine Dyes. *Inorg. Chem.* **2022**, *61*, 18850–18860.
(49) Alías-Rodríguez, M.; Bhattacharyya, S.; Huix-Rotllant, M. Ultrafast Spin Crossover Photochemical Mechanism in FeII(2,2'-bipyridine)32+ Revealed by Quantum Dynamics. *J. Phys. Chem. Lett.* **2023**, *14*, 8571–8576.
(50) Juban, E. A.; Smeigh, A. L.; Monat, J. E.; McCusker, J. K. Ultrafast dynamics of ligand-field excited states. *Coord. Chem. Rev.* **2006**, *250*, 1783–1791.
(51) Figgis, B. N.; Reynolds, P. A.; White, A. H. Covalent bonding in cis-[Fe(bpy)2Cl2][FeCl4] studied by x-ray diffraction at 120 K. *Inorg. Chem.* **1985**, *24*, 3762–3770.
(52) Matsubara, Y.; Yamaguchi, T.; Hashimoto, T.; Yamaguchi, Y. Iron(II) bipyridine complexes for the cross-coupling reaction of

https://doi.org/10.1021/acscatal.6c03087
ACS Catal. XXXX, XXX, XXX–XXX

bromocyclohexane with phenylmagnesium bromide. *Polyhedron* **2017**, *128*, 198–202.
(53) Holubowitch, N. E.; Nguyen, G. Dimerization of $[Fe^{III}(bpy)_3]^{3+}$ in Aqueous Solutions: Elucidating a Mechanism Based on Historical Proposals, Electrochemical Data, and Computational Free Energy Analysis. *Inorg. Chem.* **2022**, *61*, 9541–9556.
(54) Constable, E. C.; Housecroft, C. E. The Early Years of 2,2'-Bipyridine-A Ligand in Its Own Lifetime. *Molecules* **2019**, *24*, 3951–3989.
(55) Hannonen, J.; Kiesilä, A.; Mattinen, U.; Pihko, P. M.; Peljo, P. Electrochemical characterization of redox activity and stability of various tris(2,2'-bipyridine) derived complexes of iron(II) in aqueous solutions. *J. Electroanal. Chem.* **2023**, *950*, No. 117847.
(56) Šima, J.; Makáňová, J. Photochemistry of iron (III) complexes. *Coord. Chem. Rev.* **1997**, *160*, 161–189.
(57) Figgis, B. N.; Reynolds, P. A.; Forsyth, J. B. Covalent bonding and spin density in cis-[Fe(bipy) 2 Cl 2][FeCl 4](bipy = 2,2′-bipyridyl) studied by polarised neutron diffraction. *J. Chem. Soc., Dalton Trans.* **1988**, 117–122.
(58) Nguyen, T. H.; Shannon, P.; Hoggard, P. E. Kinetics of the photooxidation of tris(bipyridine)iron(II) in chloroform. *Inorg. Chim. Acta* **1999**, *291*, 136–141.

https://doi.org/10.1021/acscatal.6c03087
ACS Catal. XXXX, XXX, XXX–XXX